The Astronomical Journal, 154:26 (7pp), 2017 July https://doi.org/10.3847/1538-3881/aa74cd

An Upper Limit on the Mass of the Circumplanetary Disk for DH Tau b*

Schuyler G. Wolff[1], François Ménard[2], Claudio Caceres[3], Charlene Lefèvre[4], Mickael Bonnefoy[2], Héctor Cánovas[5], Sébastien Maret[2], Christophe Pinte[2], Matthias R. Schreiber[6], and Gerrit van der Plas[2]

[1] Department of Physics and Astronomy, Johns Hopkins University, Baltimore, MD 21218, USA; swolff9@jh.edu
[2] Université Grenoble-Alpes, CNRS, Institut de Planétologie et d'Astrophyisque (IPAG), F-38000 Grenoble, France
[3] Departamento de Ciencias Fisicas, Facultad de Ciencias Exactas, Universidad Andres Bello. Av. Fernandez Concha 700, Las Condes, Santiago, Chile
[4] IRAM, 300 rue de la piscine, F-38406 Saint-Martin-dHères, France
[5] Departamento de Física Teórica, Universidad Autónoma de Madrid, Cantoblanco, E-28049 Madrid, Spain
[6] Instituto de Física y Astronomía, Universidad de Valparaíso, Blanco 951, Valparaso, Chile

Received 2017 March 23; revised 2017 May 16; accepted 2017 May 21; published 2017 June 27

Abstract

DH Tau is a young (~1 Myr) classical T Tauri star. It is one of the few young PMS stars known to be associated with a planetary mass companion, DH Tau b, orbiting at large separation and detected by direct imaging. DH Tau b is thought to be accreting based on copious Hα emission and exhibits variable Paschen Beta emission. NOEMA observations at 230 GHz allow us to place constraints on the disk dust mass for both DH Tau b and the primary in a regime where the disks will appear optically thin. We estimate a disk dust mass for the primary, DH Tau A of $17.2 \pm 1.7\,M_{\oplus}$, which gives a disk to star mass ratio of 0.014 (assuming the usual gas to dust mass ratio of 100 in the disk). We find a conservative disk dust mass upper limit of $0.42\,M_{\oplus}$ for DH Tau b, assuming that the disk temperature is dominated by irradiation from DH Tau b itself. Given the environment of the circumplanetary disk, variable illumination from the primary or the equilibrium temperature of the surrounding cloud would lead to even lower disk mass estimates. A MCFOST radiative transfer model, including heating of the circumplanetary disk by DH Tau b and DH Tau A, suggests that a mass-averaged disk temperature of 22 K is more realistic, resulting in a dust disk mass upper limit of $0.09\,M_{\oplus}$ for DH Tau b. We place DH Tau b in context with similar objects and discuss the consequences for planet formation models.

Key words: circumstellar matter – planetary systems – stars: individual (DH Tau)

1. Introduction

With well over 3000 confirmed extrasolar planets now known, the focus of exoplanet science is shifting from their discovery to understanding the details of their formation and evolution. However, increasing our understanding of this complex process can only be achieved with unambiguous detections of planetary mass bodies still in formation. Today, a handful of good candidates are known (Kraus & Ireland 2012; Biller et al. 2014; Reggiani et al. 2014; Quanz et al. 2015; Sallum et al. 2015), but they are still embedded deeply in the circumstellar disk and also located close to the central objects. These are challenging conditions to study the processes that lead to their formation.

Fortunately, a small population of planetary mass companions (PMCs) has recently been discovered that offers a much better opportunity to study the planet formation process in greater detail with current instruments. These PMCs, identified by direct imaging surveys in the NIR, orbit very young host stars (T Tauri stars) and they do so at large enough separations to be easily observable, typically several hundred au (~1 arcsec; e.g., Neuhäuser et al. 2005; Lafrenière et al. 2008; Schmidt et al. 2008; Ireland et al. 2011; Bailey et al. 2014).

While planets at separations of <100 au are thought to be the consequence of either core accretion (Lissauer & Stevenson 2007) or gravitational instabilities (Boss 1997, 2011) acting at the Class II stage (i.e., T Tauri stage), planets at larger separations are believed to be products of disk fragmentation at an earlier stage (Class 0 or I stage, Kratter et al. 2010). All of these mechanisms require that a forming planet builds up from its own circumplanetary disk that formed either from the surrounding cloud, or from the massive disk around the host star. Indirect evidence for the presence of such disks is provided by the fact that planet-mass companions in young systems are powerful Hα emitters, e.g., OTS 44, GSC 06214-00210 b, GQ Lupi b, FW Tau c, and DH Tau b (Joergens et al. 2013; Zhou et al. 2014). The Hα emission, or some portion of it, being the trace of accretion from the disk onto the companion. The more direct detectability of these circumplanetary disks was recently demonstrated when ALMA measured the continuum and CO emission around the PMC orbiting the TTauri binary FW Tau (Caceres et al. 2015). The disk around FW Tau C (the PMC) has an estimated disk mass of 2–3 $M_{\oplus}$. Attempts have been made to resolve the circumplanetary disks around several other PMCs with radio interferometry (e.g., GSC 0614-210 B; Bowler et al. 2015, GQ Lupi; Dai et al. 2010, MacGregor et al. 2016), but no other detections exist to date.

2. The DH Tau System

DH Tau is a binary system with a projected separation of 330 au (2.″3). The system is located in the Taurus star-forming region at a distance of 140 pc, with an extinction in the J band of $A_J = 0.3 \pm 0.3$ (Itoh et al. 2005), and a mean age of 2.3 Myr (Bertout et al. 2007). The primary is a classical T Tauri star with an M1Ve spectral type (Herbig 1977) with $\log(T/K) = 3.5688 \pm 0.0170$ and $\log(L/L_{\odot}) = -0.262 \pm 0.110$ (Andrews et al. 2013). DH Tau b was initially discovered

* This work is based on observations carried out under project D15AC with the IRAM NOEMA Interferometer. IRAM is supported by INSU/CNRS (France), MPG (Germany), and IGN (Spain).

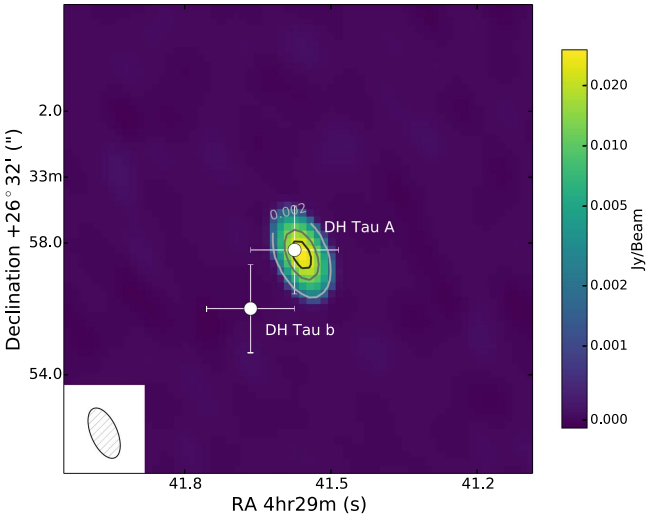

Figure 1. 1.3 mm continuum NOEMA observations of the DH Tau system. The disk of DH Tau A is clearly detected, but is unresolved. The disk of DH Tau b is undetected. Contours are drawn beginning at 0.002 Jy beam^{-1} in intervals of 0.01 Jy beam^{-1}. The errors in the positions of the DH Tau A and b components are dominated by the proper motion uncertainties. The symmetric sidelobes are an artifact of the baseline configuration. The inset shows the beam with a PA of 27.°8, a major axis of 1.″61, and a minor axis of 0.″79.

by Itoh et al. (2005), who classified it as an L2 spectral type brown dwarf with a mass of 30–50 $M_{\rm Jup}$. Luhman et al. (2006) later compared bolometric luminosities to updated evolutionary tracks and gave a revised mass estimate of 11^{+10}_{-3} $M_{\rm Jup}$, placing it near the exoplanet/brown dwarf boundary. Patience et al. (2012) modeled the atmosphere using *J, H,* and *K* spectra, and inferred a radius for DH Tau b of $2.7 \pm 0.8\,R_{\rm Jup}$, and a temperature of 2350 ± 150 K. Bonnefoy et al. (2014) give a spectral type for DH Tau b of M9.25 $\pm$ 0.25 (corresponding to 15 $M_{\rm Jup}$).

DH Tau b is the youngest PMC known to date. It is known to be actively accreting, as traced by very strong Hα emission (Zhou et al. 2014). The Pa β line of hydrogen is also reported, in emission, by Bonnefoy et al. (2014) further supporting the idea that DH Tau b is still accreting. DH Tau as a system also displays unresolved MIR excess, which, given the accreting nature of DH Tau b, is likely caused in part by the circumplanetary disk. Harris et al. (2012) reported a 47 mJy detection around the DH Tau primary at 0.88 mm. Their observations with the SMA only provided a 3σ upper limit of 10 mJy at 0.89 mm for DH Tau b. The circumplanetary disk has remained undetected to date.

In Section 3, we present the NOEMA observations of the DH Tau system and the VLT/SINFONI spectroscopy of the Pa β hydrogen line. Section 4 presents the upper limits on the disk mass of DH Tau b, an estimated disk mass for DH Tau A, and the disk model used. Finally, in Section 5, we discuss the disk mass results and place them in context with other observations of circumplanetary disks.

3. Observations

3.1. NOEMA 1.3 mm Continuum Imaging

The data presented in Figure 1 were obtained with NOEMA, the NOrthern Extended Millimeter Array. The observations were carried out on 2015 December 10th. At that time, the array was in the 7C compact configuration, with 6 antennas operating. Station W09 was off-line. Antennas were based on stations E12, N17, N11, E18, W12, and E04. The resulting 15 baselines ranged from 48 to 240 m in length (unprojected). DH Tau and its companion were observed for a total of 6.5 hr between hour angle -0.3 and $+6.0$ hr, of which we spent 4.5 hr on-source. The rest of the time was used for calibration.

We used 0400+258 and 0507+179 as phase calibrators. The atmospheric conditions were excellent and the rms phase noise was measured between 12° on short baselines and 29° on long baselines, at 1.3 mm. This phase noise introduces a position error of less than 0.1 arcsec. The source LkHa 101 was used for the flux calibration, while 3C84 was used for the bandpass calibration. We consider an absolute flux uncertainty of 10%. The total bandpass for the 230.5 GHz continuum measurement was 3.2 GHz in each polarization. We excluded a short range (80 MHz) that included the CO(2-1) line. The GILDAS software package was used to reduce the data.

The continuum map was produced using natural weighting of the visibilities to favor signal-to-noise over angular resolution. The resulting beam size is 1.″61 × 0.″79 at P.A. 28°. High signal-to-noise on DH Tau A allows for phase self-calibration. This allowed us to correctly remove sidelobes that remained present after the first reduction steps. We do not perform amplitude self-calibration in order to preserve the absolute flux measurement. The phase self-calibration stopping criteria was set to 1000 iterations. From the visibilities, we compute the stable thermal noise limit (absolute flux limit) to be 0.0653 mJy. Any residuals after self-calibration correspond to a lack of uv coverage that is impossible to correct.

We find a 1σ flux limit of 0.0653 mJy beam^{-1} for the 1.3 mm continuum data, which corresponds to a 3σ upper limit for the DH Tau b circumplanetary disk flux of 0.196 mJy. Primary beam attenuation was not taken into account because of the small separation between DH Tau A and DH Tau b (beam attenuation <2% at the position of DH Tau b). We detect the central component of the system, DH Tau A, at >100σ, with an integrated disk flux of 30.8 $\pm$ 0.2 mJy.

3.2. VLT/SINFONI Spectroscopy of the Paschen β Hydrogen Line

DH Tau b was observed with the VLT/SINFONI instrument on 2007 October 25th, November 7th, December 16th, and December 18th (program ID 080.C-0590(A)). SINFONI is composed of an integral field spectrograph SPIFFI fed by the adaptive optics module MACAO (Eisenhauer et al. 2003; Bonnet et al. 2004). The instrument was operated with the J-band grating yielding a spectral resolution of ~2000 over the 1.1–1.35 μm range. The pre-optics was sampling the 0.″8 × 0.″8 field of view with a spaxel size on the sky of 12.5 × 25 mas. Each sequence is composed of 8 × 300 s exposures with small dithering and one acquisition on the sky at the end to ensure a proper removal of the sky emission. Telluric standard stars were observed after DH Tau on each night to estimate the contamination by telluric features in the companion spectra. Because the Paschen β line is not significantly affected by telluric lines in our spectra, we decided not to correct for telluric features in order to avoid adding noise to our spectra. The October, November, and December 16 data were published in Bonnefoy et al. (2014). We reduced the December 18 data with the same tools as used in Bonnefoy et al. (2014) in order to get a homogeneous set of extracted spectra of the companion.

Table 1
Equivalent Width of the Paschen β Line

MJD Date—245000	S/N	Equation Width (Å)
4398.5	16	-1.17 ± 0.38
4411.5	18	-2.11 ± 0.40
4450.5	20	0.16 ± 0.24
4452.5	19	-0.67 ± 0.32

A Paschen β emission line is detected in the November observations, marginally detected in October, and not detected in December. All spectra have a comparable estimated S/N between 1.29 and 1.31 μm.[7] We estimated the equivalent width of the line following the method of Sembach & Savage (1992). The continuum was estimated in a range adjacent to the line, between 1.277 and 1.281 μm, and between 1.283 and 1.287 μm. The equivalent width is computed between 1.281 and 1.283 μm. The values are reported in Table 1 and their evolution in time is shown in Figure 2.

Assuming the Pa β line in emission is tracing accretion of material onto DH Tau b, then the results presented in Table 1 and Figure 2 provide indications that the accretion process itself may be variable in time. This is reminiscent of the well documented variability of the accretion process in more massive T Tauri stars, e.g., Sousa et al. (2016). The poor time coverage for the spectral variations of DH Tau b forbids a deeper analysis. We do not discuss further the variability of accretion in DH Tau b, but note it is very likely present.

4. Circumplanetary Disk Models and Results

In this section, we present models for the dust mass estimates extracted from the 1.3 mm continuum NOEMA data. We will consider three cases: the disk of DH Tau b is heated by DH Tau b only; the disk is heated by DH Tau A; and the disk is in equilibrium with the ambient cloud (assumed at 20 K). To test the dominant source of the disk dust temperature, we combine the contributions from DH Tau A and DH Tau b using a radiative transfer model.

We expect the disk to be optically thin at 1.3 mm. In this case, the disk dust mass can be expressed as

$$M_{\rm dust} = \frac{F_\nu D^2}{\kappa_\nu B_\nu(T_{\rm disk})}$$

where F_ν is our measured $\nu = 230$ GHz (1.3 mm) 3σ flux limit, D is the distance (140 pc), κ_ν is the dust opacity, and $B_\nu(T_{\rm dust})$ is the Planck function evaluated at the disk temperature. We use the dust opacity law from Beckwith et al. (1990); $\kappa_\nu = 10\,(\nu/10^{12}\,{\rm Hz})^\beta\ {\rm cm^2\ g^{-1}} = 2.3\ {\rm cm^2\ g^{-1}}$ for frequency, ν, and power-law index, $\beta = 1$.

Typical disk temperatures are ~20 K, but this varies with stellar luminosity. For DH Tau b, we calculate a luminosity of 0.0021 $L_\odot$ using the radius and stellar temperature (Zhou et al. 2014). van der Plas et al. (2016) provide a scaling relation between stellar luminosity and disk temperature for low-mass stars; $T_{\rm disk} = 22(L/L_\odot)^{0.16}$ K, which gives a disk temperature for DH Tau b of 8.2 K.

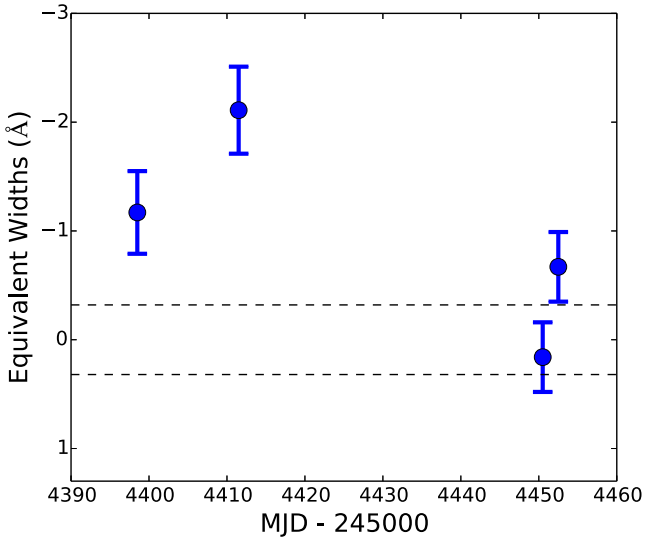

Figure 2. Variability of the Pa β equivalent width with time provides further evidence of an accreting circumplanetary disk surrounding DH Tau b. The dashed lines represents the mean 1σ error for the equivalent width measurements.

It is worth noting here that the temperature of molecular clouds is typically in the range of 10–20 K (Goldsmith 1987). In this case, the temperature of the disk may depend more on the ambient temperature from the Taurus SFR than the central source. Likewise, DH Tau b is located nearby to the much more luminous DH Tau A primary, with a luminosity of 0.55 $L_\odot$ and an effective stellar temperature of $T_* = 3706$ K (Andrews et al. 2013). If we treat the dust as a black body in thermal equilibrium with the central star, DH Tau A, at the distance of DH Tau b (330 au) with a circumplanetary disk albedo of a = 0.5, we expect the equilibrium temperature to be $T = T_*(1-a)^{1/4}\sqrt{R_*/2D} = 11$ K. Depending on the orientation of the disk relative to the central star and/or the optical depth of the disk, there could be some additional heating due to illumination from the primary, DH Tau A. Viscous heating due to accretion could also raise the temperature of the disk and serve as another source of uncertainty in the dust mass estimate.

We reproduce the effect of the host star on the disk dust temperature by generating an MCFOST radiative transfer model of the system (Pinte et al. 2006, 2009). MCFOST is a Monte Carlo Radiative Transfer code designed to study circumstellar disks. At each grid location in the modeled disk, the temperature and scattering source function are computed via a Monte Carlo method: photon packets are propagated stochastically through the model volume following the equations of radiative transfer. MCFOST allows the user to include multiple radiative sources, allowing the inclusion of the DH Tau A primary located 330 au from the circumplanetary disk. DH Tau A was modeled using an effective temperature of 3700 K and a low surface gravity of $\log(g) = 3.5$, while DH Tau b was assumed to have an effective temperature of 2300 K with $\log(g) = 3.5$. For DH Tau b, we assume an axisymmetric disk model with a gas supported flaring exponent of 1.125, and a surface density described by a power law in radius with an index of −0.5. The grains are comprised of astronomical silicates with a grain size distribution defined by an ISM-like

[7] The S/N was computed in a two step process. We first interpolated the IRTF spectrum of the M9 dwarf LP 944-20 on the SINFONI wavelength grid and normalized it in flux to the flux of the pseudo-continuum of DH Tau b over the 1.29–1.31 μm range. We used this template spectrum to approximate, then remove, all the intrinsic features of the DH Tau b (FeH lines mostly) and compute the local level of the noise.

−3.5 power-law exponent and grain sizes ranging from 0.1 to 1000 μm. The resulting dust opacity is 2.29 cm^2 g^{-1}, similar to the dust opacity of 2.3 cm^2 g^{-1} predicted above for an optically thin disk. We assume a gas to dust mass ratio of 100 and a distance of 140 pc. For simplicity, DH Tau b receives light directly from DH Tau A without attenuation, as if DH Tau b was located out of plane from the disk of DH Tau A.

The typical value for the outer radius of a circumplanetary disk is not well constrained. Numerical simulations of embedded circumplanetary disks suggest that the radii truncate at a fraction of the Hill radius due to interactions with the viscous, young circumstellar disk (Ward & Canup 2010). For DH Tau b, the Hill radius is $R_{\rm Hill} = a\left(\frac{M_p}{3M_*}\right)^{1/3} \simeq 70$ au for the planetary mass and separation ($M_p = 11\,M_{\rm Jup}$, $a = 330$ au respectively) given in the Introduction, and the primary star mass (M_*) of $0.37 \pm 0.12\,M_\odot$ from Itoh et al. (2005). Alternatively, if the DH Tau b disk formed from the collapse of the surrounding cloud, it would be expected to have a larger radius. Schaefer et al. (2009) survey the disks of young, low-mass stars in the Taurus–Auriga star-forming region and find a range in disk outer radii of $R_{\rm out} \sim$ 100–1000 au from resolved CO emission. However, a larger disk would be truncated due to the presence of the primary at a ∼0.3–0.5 fraction of the 330 au separation (Papaloizou & Pringle 1977). A disk truncated at 110 au (diameter ∼ 1.″6) is roughly the same size as the beam along the major axis (1.″61). In either case, this is below the beam size, and we treat the disk as a point source in our data. For the MCFOST model, we define the disk outer radius to be the Hill radius of 70 au.

The model was tested for several disk dust masses covering the range predicted for the various dust temperatures, and for different orientations of the circumplanetary disk with respect to DH Tau A. We found that the disk orientation (e.g., face-on, edge-on, or intermediate illumination from the central star) has no measurable effect on the azimuthally averaged dust temperature. Figure 3 shows the mass-averaged temperature profile for three assumed disk masses and includes for comparison a disk model without the host star included. As the disk dust mass increases, the midplane temperature of the disk decreases as the disk becomes more opaque to radiation. In the outer regions of the disk, all MCFOST models converge on a dust disk mass-averaged temperature of 22 ± 2 K, corresponding to a disk dust mass upper limit of $0.09 \pm 0.01\,M_\oplus$. This temperature and associated mass estimate is more consistent with what is expected for a disk in a young star-forming region. We caution that assumptions in the disk model and the uncertainty in the separation of DH Tau b could result in a lower dust temperature.

Table 2 gives the estimated disk mass upper limits for DH Tau b for the various temperatures described above. On the most conservative end, we provide an upper limit on the circumplanetary disk mass of $0.42\,M_\oplus$. However, the dust disk mass can likely be constrained further given the circumplanetary environment and as suggested by radiative transfer models of the system to be $0.09\,M_\oplus$. We adopt this upper limit for future discussion.

The temperature derived disk masses quoted above assume that the disk is optically thin at the 1.3 mm wavelength. If the disk were optically thick, i.e., $\tau > 1$, where $\tau = \int \rho\kappa_\nu ds = \kappa_\nu \Sigma > 1$, then the observed flux can be used to set a lower limit on the extent of the disk. Using the dust opacity law given above with $\beta \simeq 0$ for the optically thick case, the DH Tau b disk dust mass of $0.09\,M_\oplus$, and assuming a flat surface density, we can constrain the radius of the disk: $R < \sqrt{\kappa_\nu M_D/\pi} < 2.9$ au. Therefore, if the disk were optically thick, it would have to be compact.

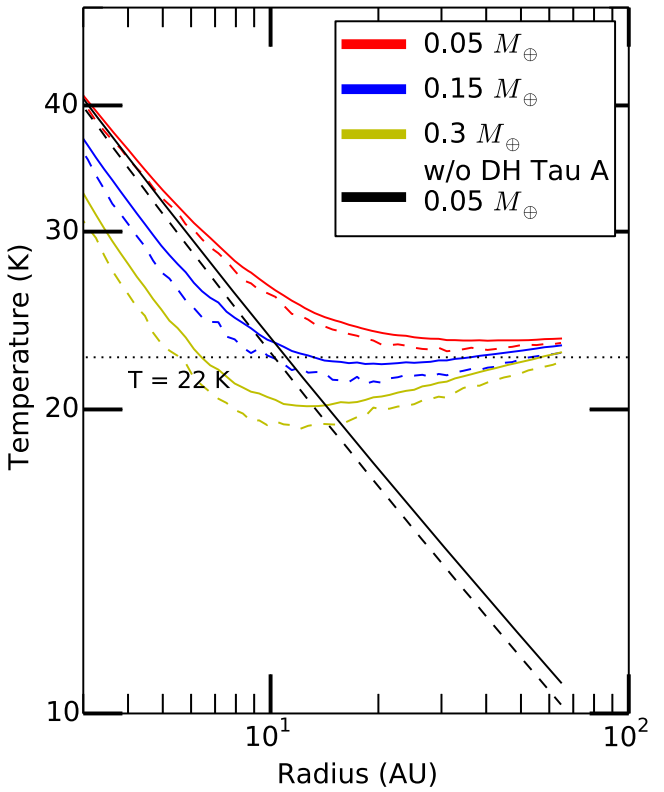

Figure 3. Dust temperature profile for the set of MCFOST radiative transfer disk models with different disk dust masses. The dashed lines show the radial profile of the disk midplane temperature, while the solid lines show the radial profile of the mass-averaged dust temperature. As the mass increases, the disk becomes more optically thick to radiation and the temperature decreases. At the outer edges of the disk, all dust mass models converge to a mass-averaged dust disk temperature of 22 K (as indicated by the dotted line).

Table 2
DH Tau b Disk Dust Mass Upper Limits

Temp.	Dust Mass Limit	Source
20 K	$0.11 \pm 0.01\,M_\oplus$	Ambient cloud temp.
8.2 K	$0.42 \pm 0.04\,M_\oplus$	DH Tau b luminosity
11 K	$0.26 \pm 0.03\,M_\oplus$	Illumination from primary
22 K	$0.09 \pm 0.01\,M_\oplus$	MCFOST model

Using the same formalism with a midplane disk temperature of 20 K as predicted from the van der Plas et al. (2016) stellar luminosity relation for low-mass stars, we estimate a disk dust mass for the primary, DH Tau A of $17.2 \pm 1.7\,M_\oplus$. The uncertainties are based on the absolute flux uncertainty and do not include errors in the assumed distance and disk opacity.

5. Discussion

We are able to place an upper limit on the circumplanetary disk mass of the DH Tau b PMC. While the dust mass limit of $0.09\,M_\oplus$ is clearly not massive enough anymore to form planets, it still provides ∼8 lunar masses of solid material to form satellites or minor bodies orbiting DH Tau b. The circumstellar disk surrounding DH Tau A has a dust mass of

17 $M_\oplus$, which is above the limit required to form giant planet cores ($\sim$10 $M_\oplus$), and could still support the formation of several terrestrial planets. The circumstellar disk mass is comparable to other Taurus disk masses for this spectral type, with a disk to star mass ratio of 0.014, assuming a gas to dust ratio of 100. The equivalent disk to star mass ratio for DH Tau b would require a total disk mass of $\sim$48 $M_\oplus$, which is not reproduced by even our most conservative detection limit for an uncharacteristically low mass-averaged dust temperature.

For DH Tau b, the mass accretion rate predicted from Hα observations is 3.2 $\times$ 10^{-12} $M_\odot$ yr^{-1} (Zhou et al. 2014). Using the disk mass limit derived from the MCFOST model gives a disk dissipation timescale of 9.1 Myr assuming a gas to dust ratio of 100.

5.1. Comparison to Known PMC Disk Masses

While there are not yet many disk mass estimates using millimeter continuum data for planetary mass objects, we compare these estimations for DH Tau b with the results for three other known wide separation PMCs: FW Tau C, GSC 6214-210 B, and GQ Lup B.

FW Tau: The FW Tau primary is actually a binary system with two M5 stars orbiting at 11 au, while the companion, FW Tau C has a mass of 7 $M_{\rm Jup}$ (Kraus et al. 2015). It is also in the Taurus SFR, with a similar age to DH Tau. Millimeter observations of the FW Tau system do not detect the circumbinary disk, but do detect the circumplanetary disk with an estimated dust mass of $\sim$2 $M_\oplus$ (Caceres et al. 2015). This dust mass is well above the average dust to stellar mass ratio for the Taurus SFR. The non-detection of the primary disk is unusual, though it is possible that the binary system caused the circumbinary disk to dissipate more quickly.

GQ Lup: GQ Lup is in the Lupus 1 SFR, with a slightly older 3 Myr age (Lombardi et al. 2008; Alcalá et al. 2014). Dai et al. (2010) conduct SMA 1.3 mm observations of GQ Lup (a young, 1 Myr old T Tauri star) and detect the primary circumstellar disk with a mass of 3 $M_{\rm Jup}$, but were unable to detect any disk signatures around the secondary component. Recently published ALMA observations (MacGregor et al. 2016) detect a compact ($R_{\rm out}$ = 59 $\pm$ 12 au) circumprimary disk with a higher dust mass estimate of $\sim$15 $M_\oplus$ from 870 μm continuum observations. The circumplanetary disk is not detected with a 3σ noise floor of 0.15 mJy beam^{-1} (equivalent to DH Tau b uncertainty) with a corresponding dust mass limit of $<$0.004 $M_\oplus$ calculated assuming that the dominant disk heating source is the primary. MacGregor et al. (2016) also obtain ^{12}CO and ^{13}CO emission showing a gas disk that extends outside of GQ Lup b. A recent multi-wavelength study of the GQ Lup system using both ALMA continuum observations and MagAO optical photometry of the companion show that the circumstellar disk of GQ Lup A is misaligned with the spin axis, possibly due to interaction with GQ Lup b (Wu et al. 2017).

GSC 0614-210: The circumplanetary disk around the 10 Myr old GSC 0614-210 B was not detected in ALMA continuum observations at 880 μm with a 3σ rms noise level of 0.22 mJy beam^{-1} (Bowler et al. 2015). This is comparable to the noise floor in these DH Tau observations, implying a similarly low disk mass ($<$0.15 $M_\oplus$). The circumstellar disk for the primary was not detected.

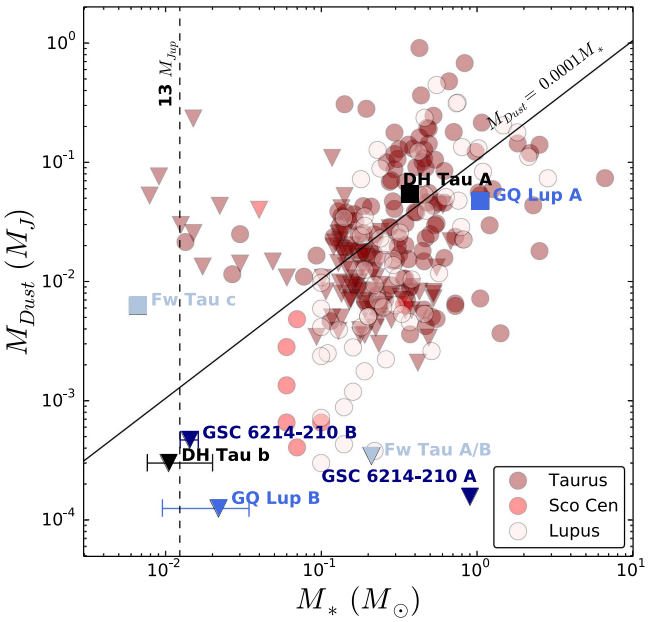

Figure 4. Disk dust mass and stellar mass are shown for a collection of labeled PMCs with dust mass estimates from millimeter observations. Dust to star mass ratios are shown in red for a collection of stars in the Taurus (Andrews et al. 2013), Lupus (Ansdell et al. 2016), and Sco Cen (van der Plas et al. 2016) star-forming regions. 3σ upper limits are represented with triangles. The dashed vertical line represents the 13 $M_{\rm Jup}$ mass deuterium burning limit, while the solid diagonal line represents a 0.0001 $M_{\rm Dust}/M_*$ ratio. The disk dust mass estimates for the PMCs are generally lower than expected for the mass of the object with the exception of FW Tau C, which has an exceptionally large dust mass.

The dust masses and stellar/planetary masses for the objects listed above are shown in Figure 4. In the event of a non-detection in the millimeter, 3σ upper limits are provided. Included for comparison are the disk dust masses and stellar masses for a collection of objects in the Taurus (Andrews et al. 2013), Lupus (Ansdell et al. 2016), and Sco Cen (van der Plas et al. 2016) star-forming regions. While the authors report the dust masses for the Lupus and Sco Cen circumstellar disks, the Taurus dust masses were computed from the provided millimeter fluxes using the stellar luminosity and temperature relation described in Andrews et al. (2013).

5.2. Formation Mechanism?

We use the ensemble of known PMCs to place constraints on the planet formation process. Different formation pathways should produce different signatures in both the accretion rates and the planet to dust disk mass ratios as compared to their environments. Here we discuss the implications of the possible formation of these wide separation PMCs.

1. Disk instability: Models of giant planets produced via disk instabilities have difficulty producing massive planet cores outside of 100 au in all but the most massive disks. Vorobyov (2013) find that a protostellar disk mass of $\simeq$0.2 $M_\odot$ is needed to produce planetary embryos with masses in the range of 3.5–43 $M_{\rm Jup}$. DH Tau A and GQ Lup A have dust disk to star mass ratios below average, while the circumstellar disks for FW Tau A/B and GSC

6214-210 A were not detected at all. As the oldest system, it is possible that the GSC 6214-210 A disk has already dissipated in its 10 Myr lifetime. However, this formation scenario is difficult to support with the current low disk mass estimates.

2. Core accretion + scattering: The most commonly employed formation mechanism for gas giant planets is via core accretion of pebbles in the parent protoplanetary disk. However, generating giant planet cores massive enough to accrete gas in situ at wide separations requires timescales longer than the lifetimes of the gas in the disk (Lissauer & Stevenson 2007). Alternatively, these planets could have been formed closer to their central stars and been dynamically scattered out to wider separations. None of the PMCs discussed here show evidence for a massive companion capable of dynamically scattering the PMC to wide separations. Indeed, direct imaging surveys of other wide separation PMCs do not find evidence for additional massive scattering companions and the core accretion + scattering event seems unlikely (e.g., Bryan et al. 2016). Surveys for scattering companions are limited by observational biases and this scenario cannot be ruled out.

   A planet formed closer in, but that has experienced such a dynamical scattering event, which would now place it at a wide separation, could potentially disrupt any circumplanetary disk. This scenario is supported by the low dust disk masses measured for all PMCs except FW Tau C, though their accretion signatures indicate that these disks are not entirely disrupted. Further monitoring of these systems to look for companions and/or signatures in their orbital properties indicative of a turbulent past could provide support to the core accretion + scattering model.
3. Turbulent fragmentation of the molecular cloud: Through the process of turbulent fragmentation, filaments within dense molecular clouds gravitationally collapse to form protostellar/planetary cores as small as a few Jupiter masses (Low & Lynden-Bell 1976). While this formation mechanism is capable of forming low-mass objects and has been invoked to explain the formation of free-floating brown dwarfs, it is difficult to produce close binaries with such extreme mass ratios such as those between a host star and a planet (Bate 2009, 2011). If the PMCs are formed from the gravitational collapse of the surrounding molecular cloud itself, and not formed in a circumstellar disk, we could expect the PMC to follow the same trend in the planet to disk mass ratio as in the parent star-forming region. However, the relative disk to star/planet-mass ratios do not appear to be correlated in binary systems, where the viscosity of the disk dictates the evolutionary timescales (e.g., Akeson & Jensen 2014; Wu et al. 2017). This mechanism is not clearly supported by the DH Tau b and GQ Lup b observations. While the circumstellar disks are detected, with median disk to stellar mass ratios indicative of a young age, the PMC disks are less massive than expected. Turbulent fragmentation is also not a good fit for FW Tau C whose disk mass is well above the disk mass for the host binary, though photoevaporation from the binary may have removed the circumbinary disk, explaining the discrepancy in the disk masses.

Accretion rates provide another valuable indicator of the formation mechanism. Bowler et al. (2011) provides a picture of accretion rates for PMCs in agreement with the accretion rate–mass relation found for low-mass stars and brown dwarfs. In fact, the reported accretion rate for GSC 0614-210 B was above average when compared to a sample of similarly low-mass brown dwarfs from Herczeg et al. (2009). Assuming these high mass accretion rates are indicative of large disk masses would seem to support formation via turbulent fragmentation. In addition, it seems that most PMCs located in young (<10 Myr), nearby star-forming regions are accreting as has been seen for field brown dwarfs (e.g., Manara et al. 2015). Evidence of circumplanetary disks from accretion signatures alone rejects core accretion and subsequent scattering as a possible formation pathway, because it would cause a disk to dissipate. If indeed future observations using a larger sample size of PMCs show that they have "normal" accretion rates for their mass but small disk masses, this could serve as a valuable marker for formation scenario.

Unfortunately, no single planet formation model is capable of explaining the observed disk masses (and upper limits) for the ensemble of known wide separation PMCs. Nonetheless, these are very exciting results because we are likely witnessing the very first stages of gaseous planet assembly. PMCs in general have the potential to offer unique insight into the early stages of extrasolar planet formation and to unveil, for the first time, the properties of circumplanetary disks. The observations of this type completed to date support discrepant formation scenarios. Millimeter continuum observations for more of these systems are required to pin down the mechanism capable of generating these massive companions at wide separations.

This material is based upon work supported by the National Science Foundation Graduate Research Fellowship under Grant No. DGE-1232825. We also acknowledge funding from ANR of France under contract number ANR-16-CE31-0013. C.C. acknowledges support from CONICYT PAI/Concurso nacional de insercion en la academia, convocatoria 2015, Folio 79150049. M.R.S. is thankful for support from the Milenium Science Initiative, Chilean Ministry of Economy, Nucleus RC 130007 and Fondecyt (1141269). H.C. acknowledges support from the Spanish Ministerio de Economía y Competitividad under grant AYA 2014-55840-P. The authors wish to thank Karl Schuster, director of IRAM, for prompt allocation of Director observing time on the NOEMA array. M.R.S. acknowledges support from Fondecyt (1141269) and the Millennium Nucleus RC130007 (Chilean Ministry of Economy). S.G.W. and F.M. thank Marshall Perrin for support and guidance in obtaining funding resources.

References

Akeson, R. L., & Jensen, E. L. N. 2014, ApJ, 784, 62
Alcalá, J. M., Natta, A., Manara, C. F., et al. 2014, A&A, 561, A2
Andrews, S. M., Rosenfeld, K. A., Kraus, A. L., & Wilner, D. J. 2013, ApJ, 771, 129
Ansdell, M., Williams, J. P., van der Marel, N., et al. 2016, ApJ, 828, 46
Bailey, V., Meshkat, T., Reiter, M., et al. 2014, ApJL, 780, L4
Bate, M. R. 2009, MNRAS, 392, 590
Bate, M. R. 2011, MNRAS, 418, 703
Beckwith, S. V. W., Sargent, A. I., Chini, R. S., & Guesten, R. 1990, AJ, 99, 924
Bertout, C., Siess, L., & Cabrit, S. 2007, A&A, 473, L21
Biller, B. A., Males, J., Rodigas, T., et al. 2014, ApJL, 792, L22
Bonnefoy, M., Chauvin, G., Lagrange, A.-M., et al. 2014, A&A, 562, A127

Bonnet, H., Conzelmann, R., Delabre, B., et al. 2004, Proc. SPIE, 5490, 130
Boss, A. P. 1997, Sci, 276, 1836
Boss, A. P. 2011, ApJ, 731, 74
Bowler, B. P., Andrews, S. M., Kraus, A. L., et al. 2015, ApJL, 805, L17
Bowler, B. P., Liu, M. C., Kraus, A. L., Mann, A. W., & Ireland, M. J. 2011, ApJ, 743, 148
Bryan, M. L., Bowler, B. P., Knutson, H. A., et al. 2016, ApJ, 827, 100
Caceres, C., Hardy, A., Schreiber, M. R., et al. 2015, ApJL, 806, L22
Dai, Y., Wilner, D. J., Andrews, S. M., & Ohashi, N. 2010, AJ, 139, 626
Eisenhauer, F., Abuter, R., Bickert, K., et al. 2003, Proc. SPIE, 4841, 1548
Goldsmith, P. F. 1987, in Interstellar Processes Vol. 134 (Dordrecht: Reidel), 51
Harris, R. J., Andrews, S. M., Wilner, D. J., & Kraus, A. L. 2012, ApJ, 751, 115
Herbig, G. H. 1977, ApJ, 214, 747
Herczeg, G. J., Cruz, K. L., & Hillenbrand, L. A. 2009, ApJ, 696, 1589
Ireland, M. J., Kraus, A., Martinache, F., Law, N., & Hillenbrand, L. A. 2011, ApJ, 726, 113
Itoh, Y., Hayashi, M., Tamura, M., et al. 2005, ApJ, 620, 984
Joergens, V., Bonnefoy, M., Liu, Y., et al. 2013, A&A, 558, L7
Kratter, K. M., Murray-Clay, R. A., & Youdin, A. N. 2010, ApJ, 710, 1375
Kraus, A. L., Andrews, S. M., Bowler, B. P., et al. 2015, ApJL, 798, L23
Kraus, A. L., & Ireland, M. J. 2012, ApJ, 745, 5
Lafrenière, D., Jayawardhana, R., & van Kerkwijk, M. H. 2008, ApJL, 689, L153
Lissauer, J. J., & Stevenson, D. J. 2007, in Protostars and Planets V, ed. B. Reipurth, D. Jewitt, & K. Keil (Tucson, AZ: Univ. Arizona Press), 591
Lombardi, M., Lada, C. J., & Alves, J. 2008, A&A, 489, 143
Low, C., & Lynden-Bell, D. 1976, MNRAS, 176, 367
Luhman, K. L., Wilson, J. C., Brandner, W., et al. 2006, ApJ, 649, 894
MacGregor, M. A., Wilner, D. J., Czekala, I., et al. 2016, arXiv:161106229M
Manara, C. F., Testi, L., Natta, A., & Alcalá, J. M. 2015, A&A, 579, A66
Neuhäuser, R., Guenther, E. W., Wuchterl, G., et al. 2005, A&A, 435, L13
Papaloizou, J., & Pringle, J. E. 1977, MNRAS, 181, 441
Patience, J., King, R. R., De Rosa, R. J., et al. 2012, A&A, 540, A85
Pinte, C., Harries, T. J., Min, M., et al. 2009, A&A, 498, 967
Pinte, C., Ménard, F., Duchêne, G., & Bastien, P. 2006, A&A, 459, 797
Quanz, S. P., Amara, A., Meyer, M. R., et al. 2015, ApJ, 807, 64
Reggiani, M., Quanz, S. P., Meyer, M. R., et al. 2014, ApJL, 792, L23
Sallum, S., Follette, K. B., Eisner, J. A., et al. 2015, Natur, 527, 342
Schaefer, G. H., Dutrey, A., Guilloteau, S., Simon, M., & White, R. J. 2009, ApJ, 701, 698
Schmidt, T. O. B., Neuhäuser, R., Seifahrt, A., et al. 2008, A&A, 491, 311
Sembach, K. R., & Savage, B. D. 1992, ApJS, 83, 147
Sousa, A. P., Alencar, S. H. P., Bouvier, J., et al. 2016, AA, 586, A47
van der Plas, G., Ménard, F., Ward-Duong, K., et al. 2016, ApJ, 819, 102
Vorobyov, E. I. 2013, A&A, 552, A129
Ward, W. R., & Canup, R. M. 2010, AJ, 140, 1168
Wu, Y.-L., Sheehan, P. D., Males, J. R., et al. 2017, ApJ, 836, 223
Zhou, Y., Herczeg, G. J., Kraus, A. L., Metchev, S., & Cruz, K. L. 2014, ApJL, 783, L17